PERGAMON

International Journal of Multiphase Flow 27 (2001) 1603–1626

International Journal of Multiphase Flow

www.elsevier.com/locate/ijmulflow

Localized force representations for particles sedimenting in Stokes flow

M.R. Maxey [a,*], B.K. Patel [b]

[a] *Center for Fluid Mechanics, Turbulence and Computation, P.O. Box 1966, Brown University, 37 Manning Street, Providence, RI 02912, USA*

[b] *Division of Engineering, Box D, Brown University, Providence, RI 02912, USA*

Received 3 June 1998; received in revised form 29 January 2001

Abstract

A finite-valued force multipole expansion is developed to describe the dynamics of spherical particles sedimenting in Stokes flow. The lowest level of the method is a simple force coupling procedure to represent the dynamic coupling between the particle phase and the fluid phase. The length scale associated with the finite force envelope provides an additional parameter that when matched to the particle size gives consistent results for the particle velocity. Sedimentation velocities for particles in a cubic lattice are predicted with good accuracy up to volume fractions of 20% by this approximate method. The calculated kinetic energy dissipation by viscosity is correctly balanced with the release of potential energy. As a full expansion procedure it is possible to calculate exactly the flow surrounding the particles, using standard numerical procedures such as fast Fourier transforms in periodic domains. Examples for the settling of particle pairs and random suspension are also given.

1. Introduction

The sedimentation of spherical particles settling in a liquid is an important and common problem in the handling of materials in manufacturing or for particle separation in many chemical, biomedical or biological systems. It has also become a canonical problem in the study of dispersed two-phase flow, providing a valuable test for simulation methods or theoretical models. In a previous paper (Maxey et al., 1997) we introduced a specific model for the motion of particle-laden flows where the equations of fluid motion are applied to the whole region, including the volume nominally occupied by the particles. The equations of motion for incompressible flow in this force-coupling model are:

* Corresponding author. Tel.: +1-401-863-1482; fax: +1-401-863-2722.
E-mail address: maxey@cfm.brown.edu (M.R. Maxey).

0301-9322/01/$ - see front matter
PII: S0301-9322(01)00014-3

$$\rho\left(\frac{\partial \mathbf{u}}{\partial t}+\mathbf{u}\cdot\nabla\mathbf{u}\right)=-\nabla p+\mu\nabla^2\mathbf{u}+\mathbf{f}(\mathbf{x},t), \tag{1}$$

$$\nabla\cdot\mathbf{u}=0, \tag{2}$$

$$\mathbf{f}(\mathbf{x},t)=\sum_{n=1}^{N}\mathbf{F}^{(n)}\Delta(\mathbf{x}-\mathbf{Y}^{(n)}(t)). \tag{3}$$

The velocity $\mathbf{V}^{(n)}(t)$ of the particle centered at $\mathbf{Y}^{(n)}(t)$ is determined by a local, spatial average of the fluid velocity $\mathbf{u}(\mathbf{x},t)$ as

$$\mathbf{V}^{(n)}(t)=\int \mathbf{u}(\mathbf{x},t)\Delta(\mathbf{x}-\mathbf{Y}^{(n)}(t))\,\mathrm{d}^3\mathbf{x}. \tag{4}$$

The presence of the particles and their action on the fluid motion is then represented by a finite, localized body force distribution (3) where the force $\mathbf{F}^{(n)}$ of the nth particle acting on the fluid is distributed over a spherically symmetric region determined by the envelope function $\Delta(\mathbf{x})$. The purpose of this paper is to develop this model in the context of Stokes flow and to demonstrate the connections between this approach and existing methods. We extend, and correct, results initially given by Maxey and Patel (1997).

Significant progress has been made towards understanding and representing the gravitational settling of small particles for which the particle Reynolds number is very low and the fluid motion around the particles is a Stokes flow. To determine the motion of a large number of rigid spherical particles in a Stokes flow one needs to determine the fluid velocity $\mathbf{u}(\mathbf{x},t)$ from

$$0=-\nabla p+\mu\nabla^2\mathbf{u}, \tag{5}$$

$$\nabla\cdot\mathbf{u}=0, \tag{6}$$

where p and μ are the fluid pressure and viscosity together with the no-slip boundary conditions on each particle surface

$$\mathbf{u}=\mathbf{V}+\Omega\times(\mathbf{x}-\mathbf{Y}). \tag{7}$$

Here $\mathbf{V}$, Ω and $\mathbf{Y}$ are the velocity, angular velocity and position vectors for the particle. This and an appropriate condition for the far field will specify the fluid motion outside the particles. An alternative is to specify a distribution of force singularities in the flow centered on each particle with the strength of each singularity chosen so as to match (7) at least approximately. This is equivalent to expressing the flow as a multipole expansion with $\mathbf{u}$ being a linear combination of Stokeslets, stresslets, rotlets, and so on for each particle, see for example Happel and Brenner (1973), Mazur and Van Saarloos (1982) and Kim and Karrila (1991).

Multipole expansions have, in one form or another, become a standard technique for the analysis of Stokes suspensions. Specific applications to issues of particle sedimentation or self-diffusion are given amongst others by Ladd (1988, 1993), Brady and Bossis (1988), Mo and Sangani (1994), Sangani and Mo (1996), Cichoki and Hinsen (1995) as well as the survey paper by Weinbaum et al. (1990). The main differences between these approaches lie in the method used to assign the multipole strengths either in terms of force densities on the particle surface or the boundary conditions (7), as well as the inclusion of lubrication forces and the order of the

multipole expansion. At the first level of approximation a multipole expansion for Stokes flow gives the point-particle representation

$$0 = -\nabla p + \mu\nabla^2\mathbf{u} + \sum_{n=1}^{N} \mathbf{F}^{(n)}\delta(\mathbf{x} - \mathbf{Y}^{(n)}) \tag{8}$$

for N particles each exerting a force $\mathbf{F}^{(n)}$ on the surrounding fluid.

A similar point-particle representation has been used too for the study of dispersed two-phase flow at finite Reynolds numbers. Squires and Eaton (1990) and Elghobashi and Truesdell (1993) have both developed numerical simulations for solid spherical particles dispersed in a turbulent gas flow to determine the extent to which the turbulence may be modified by the particle phase. The particles considered are small and either similar in size or smaller than the Kolmogorov length scale of the ambient turbulent flow. Several interesting processes have been observed regarding the damping of the turbulence by the particles and the nonuniform distribution of the particle phase.

The implementation of either a multipole expansion based on a distribution of force singularities, or a simpler point-force representation as in (8) presents several difficulties for general numerical simulations as pointed out by Maxey et al. (1997). The linearity of Stokes flow allows one to manipulate directly the flow fields generated by each force singularity term. However in a general context at finite Reynolds numbers this is not possible and the full equations of fluid motion must be solved numerically. The effect of a point singularity such as a Dirac delta function term in (8) cannot be represented accurately in a numerical scheme, be it finite difference or pseudo-spectral. Even if the particle position coincides with a computational grid point the resulting flow will not be resolved numerically and at best the results will depend on the numerical procedures used. In this paper we present an alternative procedure where a term such as the Dirac delta function $\delta(\mathbf{x} - \mathbf{Y})$ is replaced by a finite, smoothly varying function $\Delta(\mathbf{x} - \mathbf{Y})$, such as the Gaussian function

$$\Delta(\mathbf{x}) = (2\pi\sigma^2)^{-3/2}\exp(-\mathbf{x}^2/2\sigma^2). \tag{9}$$

This has the same overall effect of introducing a localized force representation. The length scale σ provides an extra parameter that may be adjusted both to ensure numerical resolution and to reflect in some way the finite size of the particle. The physical equations governing the flow are then well posed and the results should not depend on specific numerical algorithms.

A second issue that must be addressed in the simulation of sedimenting particles, using the point-particle approximation, is the particle tracking or computation of the particle motion from the local flow conditions. An individual particle will induce an infinite fluid velocity at its center, this arises from the Stokeslet singularity associated with the force the particle exerts on the surrounding fluid. Clearly this is not a physical effect and comes from using the fluid velocity at a point within the volume occupied by the particle. In a multipole expansion this is dealt with by summing the fluid velocity contributions from the particles excluding the particle in question. This procedure however cannot be adopted for finite Reynolds number simulations where it is not possible to separate the contributions from different particles. The flows generated with the localized force representations (9) are however finite at all points and this apparent difficulty with self-induced particle velocities can in fact be used to advantage as will be demonstrated later.

In the following sections of this paper we summarize the multipole expansion for Stokes flow and derive the corresponding results for an isolated particle using the localized, finite representation based on $\Delta(\mathbf{x})$. The expansion is described first as an exact calculation method where higher-order multipoles are included as necessary to ensure the boundary conditions are satisfied. A second approach is to retain only the leading-order force monopole for each particle and obtain the approximate force-coupling model for the flow. This too is described and the options for selecting the length scale associated with $\Delta(\mathbf{x})$ are discussed together with the degree that the flow outside the particle is accurately represented. In Section 5 specific examples are given for a simple cubic lattice of particles sedimenting under gravity, for the motion of a pair of particles and for a random suspension.

2. Force multipole expansions

We begin this section with a summary of the standard multipole expansion for Stokes flow as given by Saffman (1973). While there are numerous, similar versions of the multipole expansion Saffman's description provides a close comparison with the proposed finite force multipole. In both, a fluid velocity field is determined at all points, either in the fluid itself or in the volume occupied by the particle.

2.1. Singular force multipoles

The standard multipole distribution of point forces for a collection of N particles centered at $\mathbf{Y}^{(n)}$, where the index n ranges from 1 to N, results in an equation for the fluid velocity

$$0 = -\partial p/\partial x_i + \mu\nabla^2 u_i + \sum_{n=1}^{N}\{F_i^{(n)}\delta(\mathbf{x}-\mathbf{Y}^{(n)}) + F_{ij}^{(n)}\partial/\partial x_j\delta(\mathbf{x}-\mathbf{Y}^{(n)}) + F_{ijk}^{(n)}\partial^2/\partial x_j\partial x_k\delta(\mathbf{x}-\mathbf{Y}^{(n)}) + \ldots\}. \tag{10}$$

The flow is also incompressible at all points

$$\nabla\cdot\mathbf{u} = 0. \tag{11}$$

The coefficients $F_i^{(n)}$, $F_{ij}^{(n)}$, $F_{ijk}^{(n)}$ for example are the force monopole, force dipole, and force quadrupole moments. The first two are related to the fluid force and fluid torque on the nth particle, with the resultant fluid force equal to $-F_i^{(n)}$ and the torque equal to $-\epsilon_{ijk}F_{jk}^{(n)}$. These and the higher-order multipole coefficients are chosen to ensure that to the required level of approximation the boundary conditions (7) are satisfied on the surface of each particle. The equations for Stokes flow are linear so the fluid velocity $\mathbf{u}(\mathbf{x})$ may be obtained by a linear superposition of the flows induced by the individual force multipole terms.

The key elements are the fundamental solution for the Laplace equation

$$\nabla^2 g = \delta(\mathbf{x}), \tag{12}$$

which written with $r = |\mathbf{x}|$ is

$$g(\mathbf{x}) = -1/4\pi r \tag{13}$$

and the Oseen operator T_{ij} for the Stokes flow induced by a single point force at the origin

$$u_i = T_{ij}F_j, \tag{14}$$

$$T_{ij} = \frac{1}{8\pi\mu}(\delta_{ij}/r + x_i x_j/r^3). \tag{15}$$

From these the flow induced by a high-order multipole is obtained by differentiation. Saffman (1973) states a number of results of this form in the notation of generalized functions, consistent with the use of the Fourier transform method. Some caution is necessary in manipulating these results. A generalized function f is defined (see for example Griffel, 1981 or Lighthill, 1958) as a linear functional that when applied to a smoothly varying test function $\phi(\mathbf{x})$ gives a simple numerical value, denoted by $\langle f, \phi\rangle$. For an ordinary function $f(\mathbf{x})$ this is defined as

$$\langle f, \phi\rangle = \int f(\mathbf{x})\phi(\mathbf{x})\,\mathrm{d}^3\mathbf{x}. \tag{16}$$

For ordinary functions also the differentiation rule is easily shown to be

$$\langle \partial f/\partial x_i, \phi\rangle = -\langle f, \partial\phi/\partial x_i\rangle \tag{17}$$

and this becomes a definition for the generalized functions as a whole. Although the fundamental solution $g(\mathbf{x})$ of (13) and the Oseen tensor are singular at the origin these singularities are integrable and the interpretation of (16) presents no difficulty. The same is true of the flow induced by the force dipole $F_{ij}^{(n)}$ which is given by the derivative of the Oseen tensor. The response to the force quadrupole however is strictly only a generalized function. For example the degenerate force quadrupole, where F_{ijk} equals $H_i\delta_{jk}$, induces a flow specified by $\nabla^2 T_{ij}$ and this is

$$u_i = \frac{1}{4\pi\mu}P\{\delta_{ij}/r^3 - 3x_i x_j/r^5\}H_j - \frac{2}{3\mu}\delta(\mathbf{x})H_i. \tag{18}$$

The notation $P\{f(\mathbf{x})\}$ is introduced here to denote the Principal Value or finite part of this function. The evaluation of the integral (16) for the function $P\{f\}$ is defined as

$$\langle P\{f\}, \phi\rangle = \int_D f(\mathbf{x})\phi(\mathbf{x})\,\mathrm{d}^3\mathbf{x}, \tag{19}$$

where the volume D includes all points except for an arbitrarily small sphere centered on the origin where f is singular. The flow u_i given by (18) is formally incompressible at all points, but while it may appear to correspond to an irrotational source-dipole it is in fact not irrotational at the origin.

The fluid motion due to a single isolated sphere of radius a, placed at the origin and moving at velocity $\mathbf{V}$ without rotation in otherwise still fluid, is represented by a combination of a point force and a degenerate force quadrupole

$$F_i = 6\pi a\mu V_i, \tag{20}$$

$$F_{ijk} = (a^2/6)F_i\delta_{jk}. \tag{21}$$

The fluid velocity and pressure (after a minor correction) as given by Saffman (1973) are

$$u_i = \frac{1}{8\pi\mu}(\delta_{ij}/r + x_i x_j/r^3)F_j + \frac{a^2}{24\pi\mu}P\{\delta_{ij}/r^3 - 3x_i x_j/r^5\}F_j - \frac{a^2}{9\mu}\delta(\mathbf{x})F_i, \tag{22}$$

$$p = \frac{1}{4\pi}(x_i F_i/r^3) + \frac{a^2}{6}F_i\frac{\partial}{\partial x_i}\delta(\mathbf{x}). \tag{23}$$

The velocity on the sphere's surface, $r = a$, is then identically equal to $\mathbf{V}$ with these two terms. Of the contributions to the pressure in (23), the first term is $\mathbf{F}\cdot\nabla g$ associated with the force monopole, the second is due to the degenerate force quadrupole. In general the strict force multipole method (10) requires a moment of degree two higher than the force, torque or other specified term to satisfy such boundary conditions.

2.2. Finite force multipole

Once the singular Dirac delta functions $\delta(\mathbf{x}-\mathbf{Y})$ in (10) are replaced by the finite, localized force envelopes $\Delta(\mathbf{x}-\mathbf{Y})$ the procedures are in fact significantly simpler. All flow variables remain finite and nonsingular, and may be dealt with by standard methods. The Gaussian function (9) is chosen for convenience and from it analytical results can be derived for the various flow components. The key elements are again to obtain the corresponding fundamental solution for Laplace's equation and the Oseen operator for the flow induced by a localized force monopole. Corresponding to (12) the solution to

$$\nabla^2 G = \Delta(\mathbf{x}) \tag{24}$$

depends only on the radial distance r from the origin. In terms of a Fourier transform

$$\hat{G}(\mathbf{k}) = (2\pi)^{-3}\int G(\mathbf{x})\mathrm{e}^{-\mathrm{i}\mathbf{k}\cdot\mathbf{x}}\,\mathrm{d}^3\mathbf{x}, \tag{25}$$

the solution to (24) is

$$-k^2\hat{G}(\mathbf{k}) = (2\pi)^{-3}\exp(-k^2\sigma^2/2). \tag{26}$$

On the assumption that $G(r)$ tends to zero at large distances,

$$G(r) = -\frac{1}{4\pi r}\mathrm{erf}\left(\frac{r}{\sigma\sqrt{2}}\right) \tag{27}$$

and

$$\frac{\mathrm{d}G}{\mathrm{d}r} = \frac{1}{4\pi r^2}\left[\mathrm{erf}\left(\frac{r}{\sigma\sqrt{2}}\right) - (r/\sigma)(2/\pi)^{1/2}\exp\left(-\frac{r^2}{2\sigma^2}\right)\right]. \tag{28}$$

Clearly for larger values of r/σ the values of G and $\mathrm{d}G/\mathrm{d}r$ match the point representation g and $\mathrm{d}g/\mathrm{d}r$. At $r = 0$ the values are finite with $\mathrm{d}G/\mathrm{d}r$ equal to zero and

$$G(0) = -(2\pi)^{-3/2}\sigma^{-1}. \tag{29}$$

For any sphere of some given radius, centered at the origin, the net radial flux ∇G across the surface matches the volume integral of the source strength $\Delta(\mathbf{x})$ contained within the sphere.

The flow induced by a force monopole of strength **F** at the origin satisfies

$$0 = -\nabla p + \mu\nabla^2\mathbf{u} + \mathbf{F}\Delta(\mathbf{x}). \tag{30}$$

As a Fourier transform the resulting incompressible flow is

$$\hat{u}_i = (\mu k^2)^{-1}[\delta_{ij} - k_i k_j/k^2](2\pi)^{-3}\mathrm{e}^{-k^2\sigma^2/2}F_j, \tag{31}$$

so that the corresponding Oseen operator S_{ij}, where $u_i = S_{ij}F_j$, has the corresponding Fourier transform

$$\hat{S}_{ij} = \frac{1}{\mu k^2}[\delta_{ij} - k_i k_j/k^2](2\pi)^{-3}\mathrm{e}^{-k^2\sigma^2/2}. \tag{32}$$

This tensor has an isotropic dependency on the position **x** and may be written as

$$S_{ij} = A(r)\delta_{ij} + B(r)x_i x_j. \tag{33}$$

Two conditions make it possible to determine the scalar functions A and B without detailed calculations. The first is that the trace of S_{ij}, equal to $(3A + r^2B)$ must match the trace of $\hat{S}_{ij}$ which is equal to $2(\mu k^2)^{-1}\hat{\Delta}(k)$ and so

$$3A + r^2B = -\frac{2}{\mu}G(r). \tag{34}$$

The second is that the divergence of S_{ij} is zero and so the derivatives A', B' are related by

$$A' + r^2B' + 4rB = 0. \tag{35}$$

From these two conditions and the fact that neither A or B are singular at the origin

$$r^5B(r) = \frac{1}{\mu}\int_0^r s^3G'(s)\,\mathrm{d}s \tag{36}$$

and hence

$$B(r) = \frac{1}{8\pi\mu}r^{-3}\left[(1 - 3\sigma^2/r^2)\mathrm{erf}\left(r/\sigma\sqrt{2}\right) + (6\sigma/r)(2\pi)^{-1/2}\mathrm{e}^{-r^2/2\sigma^2}\right], \tag{37}$$

while

$$A(r) = \frac{1}{8\pi\mu}r^{-1}\left[(1 + \sigma^2/r^2)\mathrm{erf}\left(r/\sigma\sqrt{2}\right) - (2\sigma/r)(2\pi)^{-1/2}\mathrm{e}^{-r^2/2\sigma^2}\right]. \tag{38}$$

For large values of r/σ these functions and S_{ij} of (33), match the standard Oseen operator T_{ij}, while at the origin both A and B are finite

$$A(0) = \frac{1}{3\pi\mu\sigma}(2\pi)^{-1/2}, \quad B(0) = \frac{1}{30\pi\mu\sigma^3}(2\pi)^{-1/2}. \tag{39}$$

The new Oseen operator S_{ij} is the sum of three component parts, $S_{ij}^{(1)} + S_{ij}^{(2)} + S_{ij}^{(3)}$, with the first

$$S_{ij}^{(1)} = \frac{1}{8\pi\mu r}(\delta_{ij} + x_i x_j/r^2)\mathrm{erf}\left(r/\sigma\sqrt{2}\right), \tag{40a}$$

the second is

$$S_{ij}^{(2)} = \frac{1}{8\pi\mu}(\delta_{ij}/r^3 - 3x_i x_j/r^5)\sigma^2 \mathrm{erf}\left(r/\sigma\sqrt{2}\right), \tag{40b}$$

and the third is

$$S_{ij}^{(3)} = -\frac{\sigma^2}{2\mu}(\delta_{ij} - 3x_i x_j/r^2)\left(\frac{\sigma}{r}\right)^2 \Delta(\mathbf{x}). \tag{40c}$$

For distances r/σ large enough that $\mathrm{erf}\left(r/\sigma\sqrt{2}\right)$ is approximately one the first two components $S^{(1)}, S^{(2)}$ correspond, respectively, to a standard Oseen tensor for a point force at the origin and a standard degenerate force quadrupole. Some combination of this form is to be expected with the spherically symmetric, finite but localized distribution of the forcing in the flow.

One effect of the force monopole is to generate an axisymmetric vorticity field which satisfies a Poisson equation

$$\mu\nabla^2\boldsymbol{\omega} = -\nabla \times (\mathbf{F}\Delta(\mathbf{x})). \tag{41}$$

This vorticity is found from the transform of (41) and the fundamental solution $G(r)$ as

$$\boldsymbol{\omega} = -\frac{1}{\mu}\mathbf{F} \times \nabla G = -\frac{\mathbf{F} \times \mathbf{x}}{\mu r} G'(r). \tag{42}$$

At the origin this vorticity is zero, as it is along the axis parallel to $\mathbf{F}$, and once r/σ is large enough that $\mathrm{erf}\left(r/\sigma\sqrt{2}\right)$ is nearly equal to unity the vorticity field is the same as that generated by a point force of the same strength. Finally the pressure field associated with the force monopole is simply

$$p = \mathbf{F} \cdot \nabla G. \tag{43}$$

With these basic results one may then derive the flow induced by higher order force multipoles by differentiation of the modified Oseen operator S_{ij} or by algebraic manipulation of the Fourier transforms. An arbitrary uniform flow or a flow with a uniform velocity gradient may be added to any Stokes flow satisfying (30) without changing the balance of terms in (30). A standard assumption or normalization is used here that all flows induced by the force monopoles at the origin decrease to zero at large distances. Due to its significance for the motion of an isolated spherical particle it is of value to examine briefly the flow response to a degenerate force quadrupole as represented by the localized force envelope.

As with (18) the force quadrupole is $H_i\delta_{jk}$ and the flow is determined from the multipole expansion (10) except that the Dirac delta function is replaced by $\Delta(\mathbf{x})$. The Fourier transform for the incompressible flow response is

$$\hat{u}_i = -\frac{1}{\mu}[\delta_{ij} - k_i k_j/k^2]H_j\hat{\Delta}(\mathbf{k}). \tag{44}$$

Again, as for the singular multipole (18), this flow is not irrotational. The vorticity associated with this flow is $((1/\mu)\mathbf{H} \times \nabla)\Delta(\mathbf{x})$ and the flow field itself is given by the inverse of the transform (44),

$$u_i = \frac{1}{\mu}H_j\frac{\partial^2 G}{\partial x_i \partial x_j} - \frac{1}{\mu}H_i\Delta \tag{45}$$

or in explicit form

$$u_i = \frac{1}{4\pi\mu r^3}\left[\delta_{ij} - \frac{3x_i x_j}{r^2}\right] H_j \mathrm{erf}\left(\frac{r}{\sigma\sqrt{2}}\right) - \frac{1}{\mu}\left[\left(\delta_{ij} - \frac{x_i x_j}{r^2}\right) + \left(\delta_{ij} - \frac{3x_i x_j}{r^2}\right)\left(\frac{\sigma}{r}\right)^2\right] H_j \Delta(\mathbf{x}). \quad (46)$$

The degenerate force quadrupole produces a pressure distribution

$$p = (\mathbf{H}\cdot\nabla)\Delta(\mathbf{x}). \quad (47)$$

These results may be compared with the corresponding expressions given previously for the singular multipole expansion. The underlying pattern is the same, though now the physical variables remain finite and vary continuously. The flow (46) for the force quadrupole is equivalent to a potential flow, source-dipole in its influence at locations away from the origin and diminishes as $O(r^{-3})$. At the origin the fluid velocity is

$$-\frac{2}{3}(2\pi)^{-3/2}(\mu\sigma^3)^{-1}\mathbf{H}. \quad (48)$$

Unlike the modified Oseen tensor (40a)–(40c), which has both a Stokeslet and a force quadrupole type of response, there is no other long-range influence of this flow.

A final comment is needed about the overall force balance in a Stokes flow generated by a force monopole as in (30). No other force multipole term produces a resultant net force on the flow yet an integral of (30) over some large volume shows that the resultant force **F** must be balanced by the fluid stresses summed over the bounding volume surface. Equivalently the Fourier transform of (30) shows that there is an imbalance of the terms at zero wavenumber since both the pressure and the viscous term vanish at zero wavenumber while the force term is nonzero. One possibility might be to impose a mean, uniform pressure gradient to balance the resultant force and this normalization will be adopted for the later discussion of periodic systems of particles. For an isolated particle in a fluid of "infinite" extent this is not feasible. The balance must come either from stresses on a bounding container wall or else from a low, but nonzero Reynolds number inertial correction to the far field flow dynamics.

3. Multipole expansion for an isolated particle

The results for the finite force multipoles may be used in several different ways. First we will consider the balance of localized force distributions needed to exactly represent the flow past an isolated sphere of radius a moving with velocity **V** relative to the surrounding fluid. To achieve this the length scale σ specifying the width of the force envelope must be small enough that the force distributions be completely contained within the interior of the particle. For a rigid particle moving in still fluid there is no tendency for the particle to rotate, so $\Omega = 0$, and the no-slip boundary condition (7) is that the fluid velocity **u** equals **V** at all points on the spherical surface. The force of the particle on the fluid **F** is given by (20) as the usual Stokes drag force and the flow will be represented as a combination of a force monopole (Stokeslet) (33) and a degenerate force quadrupole (45),

$$u_i(\mathbf{x}) = S_{ij}F_j + \frac{1}{\mu}H_j\frac{\partial^2 G}{\partial x_i \partial x_j} - \frac{1}{\mu}H_i\Delta \quad (49)$$

with the particle centered at the origin.

The required value of **H** depends on the value of a/σ specified. The Stokeslet contribution $S_{ij}^{(1)}$ of (40a) matches the usual results provided $\mathrm{erf}(r/\sigma\sqrt{2})$ is approximately one, and we may note that $\mathrm{erf}(x)$ has the value 0.995 for $x = 2$ converging rapidly thereafter as x increases. If the asymptotic form of (49) for $r/\sigma \gg 1$ is compared with the standard form (22) for the induced flow, the two match provided the force quadrupole term **H** satisfies

$$\frac{a^2}{24\pi\mu}\mathbf{F} = \frac{\sigma^2}{8\pi\mu}\mathbf{F} + \frac{1}{4\pi\mu}\mathbf{H}. \tag{50}$$

This condition to determine **H** will ensure that at least away from the sphere the flow is correctly represented. If $(a/\sigma) \gg 1$, then the force quadrupole strength $H_i\delta_{jk}$ is the same as (21) for the standard, singular force multipole. In general though **H** is given by

$$\mathbf{H} = \pi\mu\mathbf{V}(a^3 - 3a\sigma^2). \tag{51}$$

With **F** and **H** thus specified the fluid velocity on the surface of the spherical particle at $r = a$ is

$$u_i = V_i\mathrm{erf}\left(\frac{a}{\sigma\sqrt{2}}\right) + (2\pi)^{-1/2}\left(\frac{a}{\sigma}\right)\left(1 - \frac{1}{2}\left(\frac{a}{\sigma}\right)^2\right)\left(\delta_{ij} - \frac{x_i x_j}{a^2}\right)V_j \exp\left(-a^2/2\sigma^2\right). \tag{52}$$

The first term approximates **V** to better than 1% accuracy if (a/σ) is equal to $2\sqrt{2}$ or greater. The second term, although rapidly decaying as a/σ increases is still significant at this value. For $a/\sigma \geqslant (2.5\sqrt{2})$ the discrepancy between **u** and **V** on the particle surface is less than 1.5% and negligible for $a/\sigma \geqslant 3\sqrt{2}$. If axes are chosen so that $\mathbf{V} = (V, 0, 0)$, then the fluid velocity component u_1 may be evaluated along the streamwise and transverse axes Ox_1 and Ox_2. These are plotted in Fig. 1 for different values of a/σ with **H** specified by (51). These results show that the fluid velocities are accurately represented away from the sphere surface with the accuracy in the near region improving as a/σ is increased. With $a/\sigma = 4.0$ the vorticity contours and streamlines

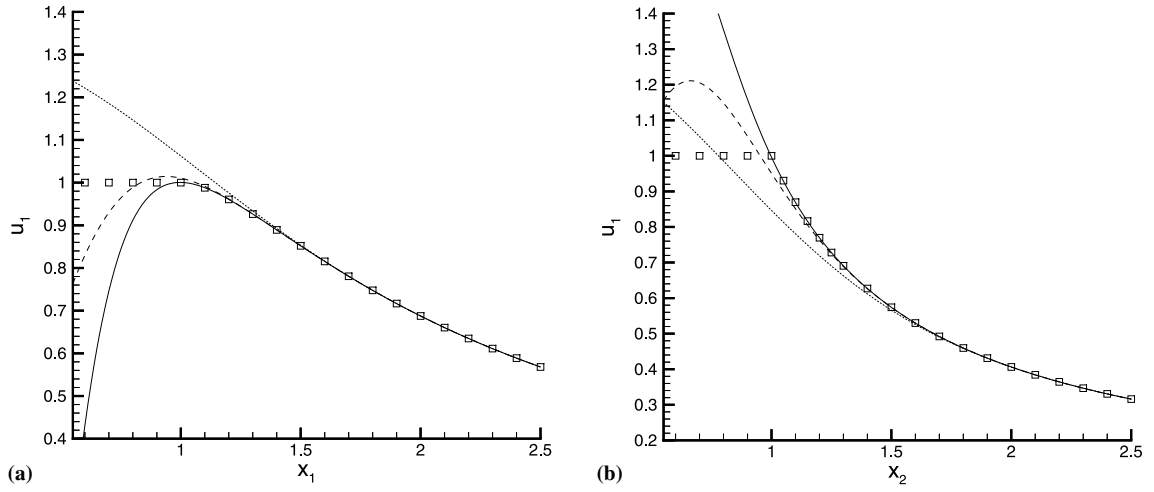

Fig. 1. Profiles of u_1 fluid velocity component along x_1-axis and x_2-axis for an isolated sphere of unit radius moving with unit velocity $(V = 1)$ in positive x_1-direction as represented by finite force multipole result (52): (. . . . . .) $a/\sigma = 2$; (- - - -) $a/\sigma = 3$; (——) $a/\sigma = 4$; and (□) Stokes flow result for a rigid sphere.

for the flow relative to the sphere given by this multipole expansion (49) are indistinguishable from the exact flow outside the sphere. The maximum surface vorticity is $1.5\ V/a$, which occurs as expected in the mid-plane $x_1 = 0$.

This approach may be applied to other flow conditions such as the motion of sphere relative to a uniform shear flow or a flow with uniform strain-rate. In the former the sphere will rotate so that the angular velocity corresponds to the imposed uniform vorticity. No net torque will act on the particle since particle inertia is considered negligible, and the force dipole coefficients F_{ij} will be symmetric. For either situation a stresslet flow is induced, while a combination of a symmetric force dipole and a degenerate force octapole will be required to match the no-slip boundary conditions on the particle. The exact correspondence between these two terms will again depend on the value of the ratio a/σ.

Clearly an accurate flow representation may be constructed through a suitable combination of these finite force multipoles for Stokes flow conditions once the particle velocity is specified and the boundary condition (7) is set. Systems of particles can be represented too following the analogous steps for standard multipole methods, see for example Brady and Bossis (1988) or Ladd (1993). If a cluster of particles is settling under gravity the external force on each particle is known and hence the strength of the force monopole term. The velocity and angular velocity of each particle in this mobility problem is determined from the flow induced by the particle motion. Force dipoles and higher-order multipoles are included as necessary to satisfy the conditions of a rigid body motion on the surface of each particle. The particle velocity is evaluated as a simple average of the fluid velocity on the particle surface, or some equivalent procedure. These issues are illustrated further in Section 5.

4. Force-coupling model

The primary focus of this paper is not to use the finite force multipoles to reproduce standard multipole solutions but rather to develop the force-coupling model (1)–(4), described briefly in the introduction, within the context of Stokes flow. The flow induced by a single moving particle or system of particles is represented approximately by retaining only the force monopole term. For spherical particles settling under gravity with no external torques the force on each particle is known and this then sets the strength of the force monopole for each particle. The issue to be resolved then is how to determine the particle velocity since the boundary conditions (7) are no longer accurately matched on the surface of each particle. A common procedure for evaluating the particle velocity $\mathbf{V}(t)$ in a dilute suspension by standard particle tracking methods (Maxey and Riley, 1983) is to assign

$$\mathbf{V} = \mathbf{u}(\mathbf{Y}, t) + \mathbf{W}, \tag{53}$$

where $\mathbf{W}$ is the Stokes settling velocity of the particle. In a Stokes suspension where the flow is represented by a singular multipole expansion (10) or point-force model (8) the value of $\mathbf{u}(\mathbf{Y}, t)$ must be calculated from the sum of the disturbance flows of each individual particle excluding the particle under consideration. This is done to avoid the infinite, self-induced fluid velocity that would result from the Stokeslet or other multipoles associated with the individual particle. A similar procedure is used by Batchelor (1972) where (53) is modified to include the Faxen

correction for the variation in the ambient flow. In contrast the finite force multipoles produce no such singularities and even at the particle center, inside the volume of fluid nominally occupied by the particle, the value of $\mathbf{u}(\mathbf{Y},t)$ remains finite. In addition the envelope scale σ is available as an extra parameter that may be chosen to meet specific requirements.

Consider first the motion of a single isolated particle settling under gravity in otherwise still fluid. The particle velocity $\mathbf{V}$ is simply the Stokes settling velocity for this particle $\mathbf{W}$. The induced disturbance flow as represented approximately by a single force monopole is

$$u_i(\mathbf{x},t) = 6\pi a\mu S_{ij}(\mathbf{x}-\mathbf{Y}(t))W_j, \tag{54}$$

where the force monopole $\mathbf{F}$ and $\mathbf{W}$ are related by the usual Stokes law (20). Evaluated at $\mathbf{Y}(t)$, the fluid velocity calculated from (33) and (39) is

$$u_i(\mathbf{Y},t) = \left(\frac{a}{\sigma}\right)\left(\frac{2}{\pi}\right)^{1/2} W_i. \tag{55}$$

The same result can also be obtained by direct integration of the Fourier transform $\hat{u}_i$ in (31). From (55) it is clear that if the envelope scale σ is chosen in relation to the particle radius such that

$$a/\sigma = (\pi/2)^{1/2}, \tag{56}$$

or approximately 1.25, then the self-induced fluid velocity at the particle's center exactly matches the Stokes settling velocity $\mathbf{W}$. To the same level of approximation then the particle tracking equation is simply

$$\mathbf{V}(t) = \mathbf{u}(\mathbf{Y},t). \tag{57}$$

Provided a/σ is set according to (56) there is no need to calculate separately the ambient flow generated by the settling of the other particles, a direct calculation of $\mathbf{u}(\mathbf{Y},t)$ suffices. In one step this eliminates the potential difficulty of the self-induced particle velocity and simplifies the calculations.

The results of the previous section have shown that as larger values of a/σ are selected the multipole representation for the flow due to a single particle is more accurate, especially in the region near the particle. As a counterpart to the results of Fig. 1 we show in Fig. 2 a comparison of the approximate fluid velocity for the disturbance flow as represented by (54) with the exact values for Stokes flow past a sphere. The correspondence is quite acceptable for $r/a > 3$ and suggests that this procedure for calculating particle velocity will be useful provided the particles remain reasonably well separated. Results for simple systems of particles based on this particle-tracking equation (57) are given by Patel (1996).

An alternative procedure is to recognize that the particles have a finite size and that they move in response to the local average fluid velocity, integrated over the particle volume. There is some arbitrariness as to how this is accomplished but a preferred choice is to define an average in terms of the envelope $\Delta(\mathbf{x}-\mathbf{Y}(t))$ itself,

$$\tilde{\mathbf{u}}(\mathbf{Y},t) = \int \mathbf{u}(\mathbf{x},t)\Delta(\mathbf{x}-\mathbf{Y}(t))\,\mathrm{d}^3\mathbf{x}. \tag{58}$$

This locally spatially averaged, or filtered, velocity has several physically valuable properties as previously noted by Maxey et al. (1997). In terms of $\tilde{\mathbf{u}}$ the particle tracking procedure is to evaluate the particle velocity as

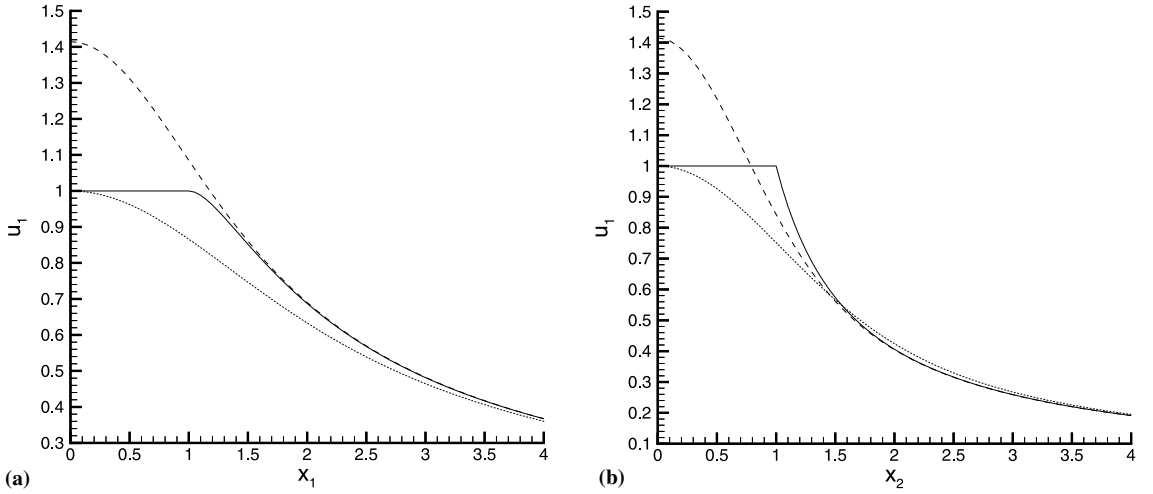

Fig. 2. Profiles of u_1 fluid velocity component along x_1-axis and x_2-axis for an isolated sphere of unit radius moving with unit velocity ($V = 1$) in positive x_1-direction as given by single force monopole result (54): (……) $a/\sigma = (\pi/2)^{0.5}$; (----) $a/\sigma = \pi^{0.5}$; and (——) Stokes flow result for a rigid sphere.

$$\mathbf{V}(t) = \tilde{\mathbf{u}}(\mathbf{Y}, t) \tag{59}$$

with the scale ratio a/σ set instead as

$$a/\sigma = \sqrt{\pi}. \tag{60}$$

As with the point velocity procedure (57) the value of $\tilde{\mathbf{u}}(\mathbf{Y}, t)$ due to a single force monopole (54) is then exactly matched to the Stokes settling velocity $\mathbf{W}$. A comparison of the profiles for the streamwise fluid velocity component for this second value of the scale ratio (60) is also shown in Fig. 2, again for the disturbance flow due to the force monopole (54). In general the correspondence with the exact Stokes flow is much closer than shown for a/σ given by (56).

The choice of $\tilde{\mathbf{u}}(\mathbf{Y}, t)$ as defined by (58) is motivated by considering the special context of an envelope $\Delta'(\mathbf{x})$ defined, for a particle centered at the origin, as

$$\begin{aligned} \Delta'(\mathbf{x}) &= 1/\Omega_\mathrm{p} \quad |\mathbf{x}| \leqslant a \\ &= 0 \qquad\quad |\mathbf{x}| > a, \end{aligned} \tag{61}$$

where Ω_p is the volume of the particle $4\pi a^3/3$. The indicator function $\chi(\mathbf{x})$ for the particle is then $\Omega_\mathrm{p}\Delta'$. If the fluid velocity satisfies the exact boundary conditions (7) on the particle surface and the flow remains incompressible in the region nominally occupied by the particle then the surface integral over the particle surface S_p

$$\oint_{S_\mathrm{p}} x_i u_j n_j \, \mathrm{d}S = V_j \oint_{S_\mathrm{p}} x_i n_j \, \mathrm{d}S, \tag{62}$$

which is equal to $\Omega_\mathrm{p} V_i$. The same surface integral may be written, by an application of Gauss' Theorem as an integral over the volume of the particle with the result that

$$\Omega_p V_i = \int u_i(\mathbf{x},t)\chi(\mathbf{x}-\mathbf{Y}(t))\,\mathrm{d}^3\mathbf{x} \tag{63}$$

and then (59) holds as an exact relationship. More generally the convolution integral (58), defined with $\Delta(\mathbf{x})$, is a smoothly varying spatial filter that approximates the particle's presence.

The main reason to select $\tilde{\mathbf{u}}$ is that a consistent energy balance may be established between the release of potential energy as a particle settles out under gravity and the viscous dissipation in the fluid. The scalar product between the fluid velocity and the equation of motion (30) for the flow induced by a single finite force monopole may be integrated over the whole region to give

$$\int \mu \frac{\partial u_i}{\partial x_j}\left(\frac{\partial u_i}{\partial x_j}+\frac{\partial u_j}{\partial x_i}\right)\mathrm{d}^3\mathbf{x} = \mathbf{F}\cdot\tilde{\mathbf{u}}. \tag{64}$$

The integral term is the complete viscous dissipation in the fluid summed over all points including the fluid volume nominally occupied by the particle. The term on the right is equal to the rate of working by the particle on the fluid provided $\mathbf{V}=\tilde{\mathbf{u}}$. In the region close to the particle, the flow field, as represented by (54), is not fully resolved and for example does not satisfy the no-slip boundary conditions. Further the rate of strain is less than in the exact flow which results in a mismatch in the local viscous dissipation. Away from the particle surface the mismatch becomes negligible. All of this is consistent with the spatial filtering associated with the finite force monopole representation at the value of $a/\sigma=\sqrt{\pi}$. To obtain a consistent estimate of the viscous dissipation within the spherical region $r<R$ this must be integrated over $0<r<R$ and not $a<r<R$ as would be done for an exact, fully resolved disturbance flow.

The flow structure corresponding to this choice of a/σ and generated by the approximate force monopole representation (54) is shown in Fig. 3. The vorticity contours have the usual general

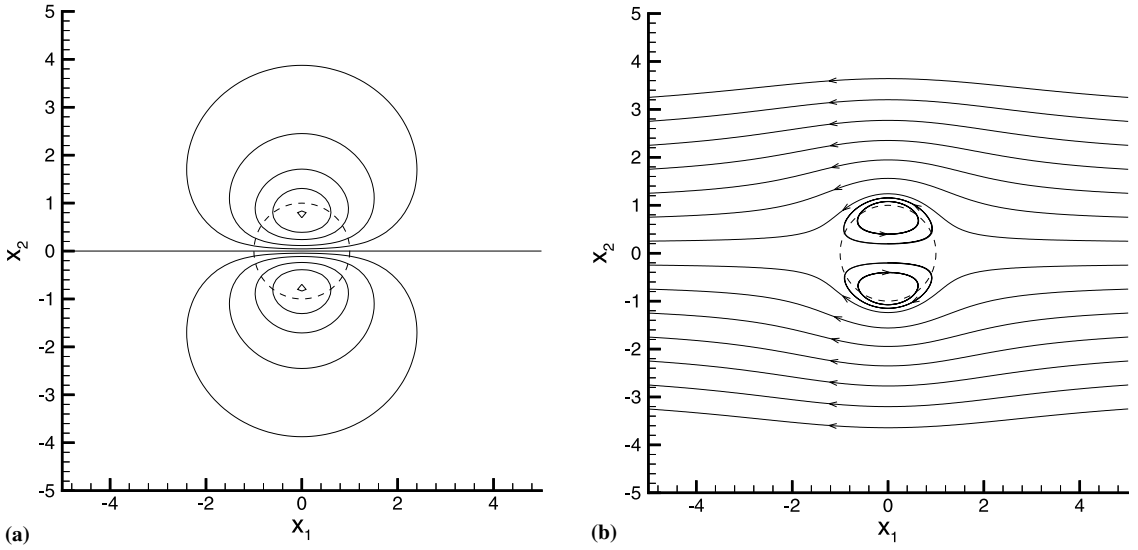

Fig. 3. Vorticity contours and steamlines calculated from the approximate single force monopole result (54) with $a/\sigma=\pi^{0.5}$. Vorticity contours are shown for $\omega_3=0$ and $\omega_3=\pm0.1$ (outermost), ±0.25, ±0.5, ±0.75, ±1.0 (innermost).

structure and closely match those of the exact flow at points away from the particle surface. The strength of the fluid vorticity near the surface is attenuated, as noted above, and the innermost vorticity contours correspond only to $\omega_3 = \pm 1.0W/a$. The peak vorticity on the surface $r = a$ is significantly less than the expected value of $1.5W/a$. The streamlines show clearly the presence of a material surface somewhat larger in radius than the actual sphere though this is not a no-slip surface for the fluid motion. There is an internal circulation within this spherical region that is similar to a Hill's spherical vortex. The open streamlines in Fig. 3 are identical to those of the exact flow except for the innermost pair in a small interval about $x_1 = 0$, near to the spherical boundary.

Some other features are worth noting about the choice of the ratio of the particle radius to the envelope scale σ. For a single isolated sphere sedimenting in otherwise still fluid the required force quadrupole strength $\mathbf{H}$ is zero if $a/\sigma = \sqrt{3}$ as specified by (51). The force monopole alone is then sufficient to generate the correct disturbance flow outside the immediate region surrounding the particle. For $a/\sigma = \sqrt{\pi}$ the value of $\mathbf{H}$ that would be appropriate is still small and this is evident in the better correspondence of the fluid velocity shown in Fig. 2. Another issue to consider with the approximate particle tracking methods such as (57) or (59) is the Faxen correction to the Stokes drag law. If an otherwise isolated particle is settling in the presence of some ambient nonuniform flow that is approximated by

$$\left(U_i^{(0)} + \frac{\partial U_i^{(0)}}{\partial x_j} x_j + \frac{1}{2} \frac{\partial^2 U_i^{(0)}}{\partial x_j \partial x_k} x_j x_k \right),$$

then the particle velocity $\mathbf{V}$ is modified and

$$\mathbf{V} = \mathbf{W} + \mathbf{U}^{(0)} + \frac{a^2}{6} \nabla^2 \mathbf{U}^{(0)}. \tag{65}$$

(See for example Happel and Brenner, 1973.) The local velocity gradient $\partial U_i^{(0)}/\partial x_j$ has no net effect on the fluid force acting on the particle while the quadratic variation modifies the particle response. Under these condition the estimate of $\mathbf{V}$ provided by $\tilde{\mathbf{u}}$ as in (59) is

$$\mathbf{V} = \mathbf{W} + \mathbf{U}^{(0)} + \frac{1}{2} \sigma^2 \nabla^2 \mathbf{U}^{(0)}. \tag{66}$$

The two expressions match if $a/\sigma = \sqrt{3}$, and agree approximately if $a/\sigma = \sqrt{\pi}$.

5. Systems of particles

5.1. Particles in a cubic lattice

The two methods based on the finite force multipoles, either the full expansion or the approximate force coupling model with only the force monopole term, are first applied to the standard problem of sedimentation for particles arranged in a simple, periodic cubic lattice. The distance between adjacent particles is L and the volume fraction c of the particles is then

$$c = 4\pi a^3/3L^3. \tag{67}$$

The particles are settling under the net force of gravity through the surrounding fluid while maintaining the cubic lattice configuration. For a Stokes flow there is no tendency for the particles to migrate out of this configuration. In isolation the particle velocity $\mathbf{V}$ equals $\mathbf{W}$, the Stokes settling velocity, which is related to the net force $\mathbf{F}^{(0)}$ due to gravity by (20). The system is maintained in equilibrium at finite volume fractions by a uniform pressure gradient that balances the net weight of the particles per unit volume. The equivalent effect is to impose a constraint of no net volume flux; the volume displacement associated with the settling of the rigid spherical particles is counterbalanced by a return flow in the surrounding fluid. The results on the change in relative settling velocity V/W with changes in volume fraction are specified in this frame of reference of no net volume flux. Alternatively the particles may be viewed as a fixed bed subject to an applied pressure gradient and then the value of V is the superficial velocity for the flow through the bed.

Hasimoto (1959) showed that at lower particle concentrations the settling velocity varies linear with the ratio of particle size to inter-particle spacing. He obtained the approximate result for the variation of V/W with concentration c,

$$V/W = 1 - 1.7601\, c^{1/3} + c - 1.5593\, c^2 + O(c^{8/3}). \tag{68}$$

Hasimoto found the flow generated by a fundamental point force in the periodic geometry and used an Ewald summation of the periodic images to obtain this result. This approach was extended by Sangani and Acrivos (1982) to obtain a more accurate estimate for the variation in V/W as well as a complete summation of the multipole expansion. They give accurate results for this variation up to the close-packing limit of $c = \pi/6$. Their results are in agreement with the calculations of Zick and Homsey (1982) who used a boundary element method for the same problem. In Fig. 4 the results of Sangani and Acrivos (1982) are compared with the results for the approximate force monopole representation (54). The flow for the periodic array of finite force multipoles is computed by fast Fourier transform methods explicitly using the periodic length scale L and a Fourier series expansion for the flow variables. Results are shown for both the point value estimate of $\mathbf{V}$ (57) with a/σ given by (56) and the local volume-averaged estimate (59) that uses $\tilde{\mathbf{u}}$ and a/σ specified by (60).

The approximate force monopole representation is in good agreement with the exact values up to values of $c^{1/3}$ equal to 0.6, or roughly $c < 0.2$. The data for higher concentrations are plotted again in Fig. 4 on an expanded scale. Even at the close packing limit the discrepancy is not large in absolute terms, approximately 0.044 compared to the correct value of 0.024. An initially surprising feature is that the approximate results for V/W are the same whether one uses $\mathbf{u}(\mathbf{Y}, t)$ or $\tilde{\mathbf{u}}(\mathbf{Y}, t)$ to calculate V, provided the ratio a/σ is set appropriately. A feature of the Gaussian function (9) used here for $\Delta(\mathbf{x} - \mathbf{Y})$ is that evaluating $\tilde{\mathbf{u}}$ is equivalent to evaluating $\mathbf{u}$ for the same force monopole but with σ^2 replaced by $2\sigma^2$. Result (55) for the induced velocity $\mathbf{u}(\mathbf{Y}, t)$ of an isolated particle is proportional to (a/σ). Even in the periodic cubic lattice the linearity of the Stokes flow problem implies a self-similarity scaling for the dependency of V/W on the combination $(a/\sigma)(\sigma/L)$, which is proportional to $c^{1/3}$.

A better understanding of the processes involved can be obtained by looking at the flow structure of a specific example. Fig. 5 shows the vorticity contours and streamlines in a symmetry plane for particles settling in the positive x_1-direction. The distance L between particles is scaled to

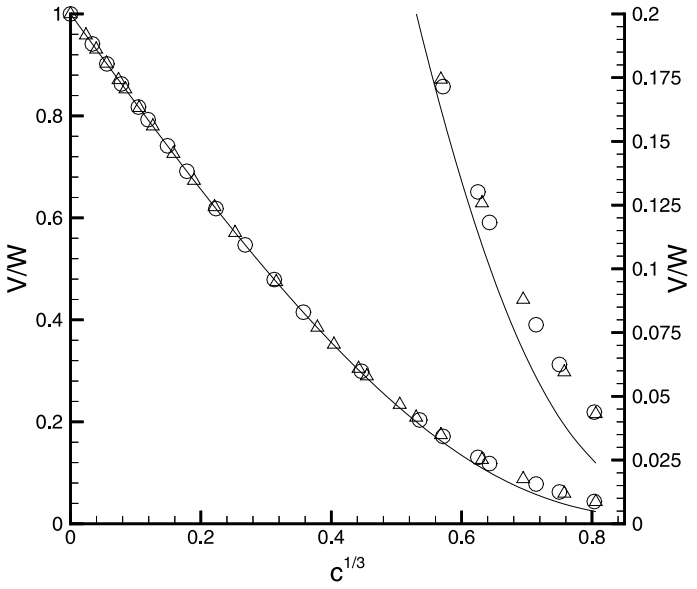

Fig. 4. Change in sedimentation velocity V of particles in a fixed simple cubic lattice as volume fraction c varies, V scaled by Stokes settling velocity W against $c^{1/3}$: (——) results of Sangani and Acrivos (1982); $(\bigcirc), a/\sigma = \pi^{0.5}; (\Delta), a/\sigma = (\pi/2)^{0.5}$.

be $L = 2$ and the corresponding particle radius is 0.375 so that $c^{1/3}$ is 0.302. The flow is calculated from the finite force multipole expansion

$$F_i^{(0)} \Delta(\mathbf{x}) + H_i \nabla^2 \Delta(\mathbf{x}) + F_{i11}^{(2)} \partial^2 / \partial x_1^2 \Delta(\mathbf{x}), \tag{69}$$

where $\mathbf{F}^{(0)} = (F^{(0)}, 0, 0)$, $\mathbf{H} = (H, 0, 0)$ and $F_{i11}^{(2)} = (F_{111}, 0, 0)$. Again the flow variables are expressed as Fourier series for the periodic array and evaluated by fast Fourier transforms. The force multipoles in (69) consist, of the usual force monopole, set by the net weight of the particle, and a degenerate force quadrupole with an additional force quadrupole term required to satisfy the flow boundary conditions on the particle surface. An extra term equivalent to a potential flow source-octapole or a degenerate force hexadecapole is also required to complete the balance of the flow boundary conditions. These terms were sufficient to ensure all boundary conditions were satisfied to an accuracy of 0.5% or better.

The vorticity contours of Fig. 5 show the internal flow structure associated with the force monopole and force quadrupole. Outside the sphere, shown by the dashed circle, the vorticity contours scaled by W/a are similar to those of an isolated sphere except they are somewhat compressed and confined by the periodic cell structure. The contours for $\omega_3 = \pm 1.5 W/a$ approximately meet the sphere surface along the symmetry line $x_1 = 0$. Indeed the maximum value for the surface vorticity is $1.538 W/a$, not significantly different from the value of $1.5 W/a$ for an isolated sphere settling with velocity **W**. This was found to be true for other concentration levels examined. The streamlines, drawn relative to the motion of the particle, show the flow around the material boundary of the sphere. The value of the required degenerate force quadrupole **H** exhibits a similar lack of sensitivity to the volume fraction. The relation (51) for **H**, with **V** set equal

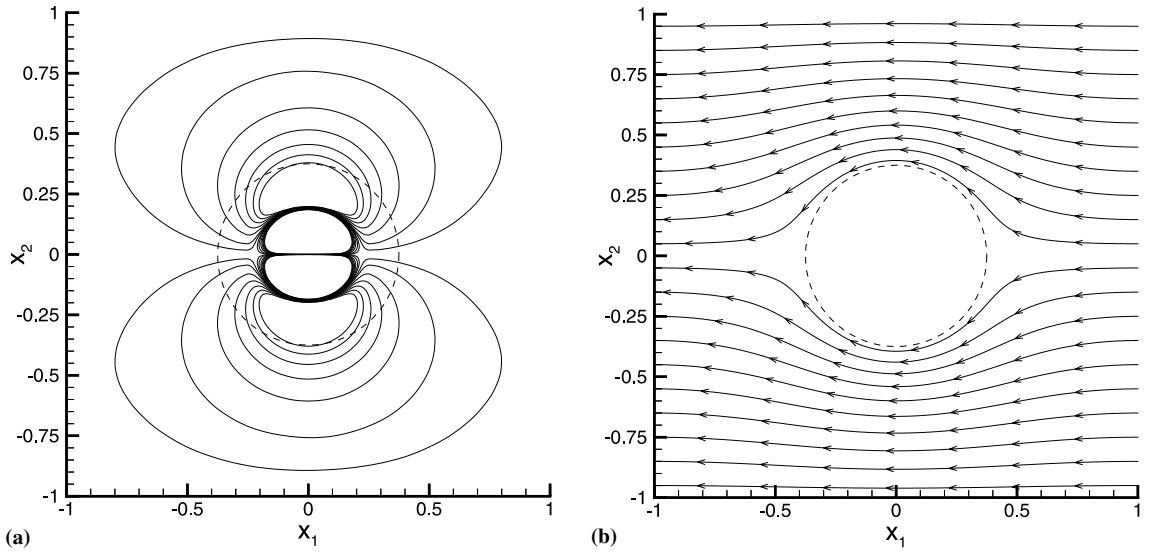

Fig. 5. Vorticity contours and streamlines for a particle in a simple cubic lattice array, calculated with finite force multipoles, shown in a symmetry plane, for $a = 0.375$. Vorticity contours shown for $\omega_3 = \pm 0.1$ (outermost), ± 0.25, ± 0.75, ± 1.0, ± 1.25 and $\pm 1.5W/a$ (inner set). Sphere is shown by the dashed circle.

to **W**, provides a good estimate of the required value. In Table 1 values are listed for the coefficients H and F_{111} in a few example cases as $c^{1/3}$ increases up to 0.6. In all cases the flow boundary conditions are satisfied to 0.5% or better except in the last example where (69) proved to be insufficient. The errors in u_1 and u_2 on the sphere in this case were ± 0.01 W relative to a value of $V/W = 0.131$.

The flow structure generated by the approximate force monopole representation for the same conditions as in Fig. 5, with $a = 0.375$ and $L = 2$, is shown in Fig. 6. The flow is matched with $\mathbf{V} = \tilde{\mathbf{u}}$ and using (59), (60). The outer vorticity contours for $\omega_3 = \pm 0.1$ and $\pm 0.25W/a$ match closely between the two sets of figures. The approximate representation has a significantly attenuated vorticity. The innermost pair of contours correspond to $\omega_3 = \pm 0.9W/a$ and the maximum surface vorticity at $r = a$ is only $0.9W/a$. This is consistent with the spatial filtering associated with the model and the limited resolution near the particle surface. The streamlines of Fig. 6 indicate as with Fig. 3 the presence of a material surface somewhat larger in size than the

Table 1
Finite force multipole coefficients for spherical particles in a simple cubic lattice[a]

a/L	$c^{1/3}$	V/W	H	H (expected)	F_{111}/H
0.125	0.202	0.651	1.25	1.24	−0.046
0.1875	0.302	0.495	4.77	4.71	−0.124
0.25	0.403	0.352	11.2	10.9	−0.266
0.3125	0.504	0.229	22.7	22.2	−0.406
0.375	0.605	0.131	37.9	37.7	−0.559

[a] The expected values of H are calculated from (51) with V set equal to W. The ratio a/σ varied between 4.0 and 8.0, viscosity $\mu = 1.0$.

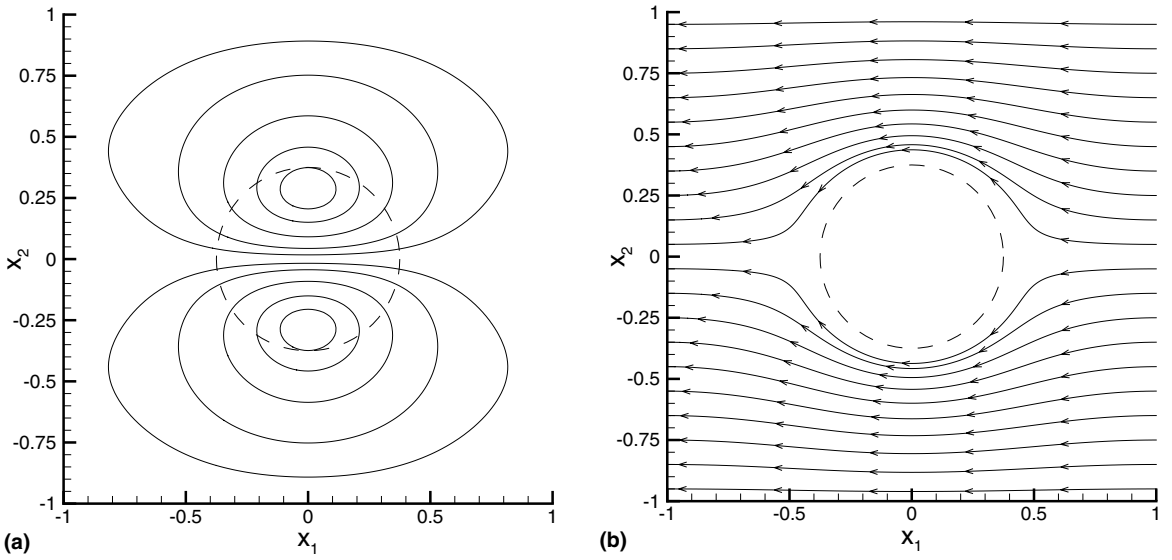

Fig. 6. Vorticity contours and streamlines, similar to Fig. 5, for $a = 0.375$, calculated with simple force monopole and $a/\sigma = \pi^{0.5}$. Vorticity contours shown for $\omega_3 = \pm 0.1$ (outermost), ± 0.25, ± 0.5, ± 0.75, $\pm 0.9W/a$ (innermost).

actual sphere. The outer streamlines match quite closely between Figs. 5 and 6 but differ noticeably close to the sphere surface.

5.2. Particle pair

A second example to consider is the motion of a pair of identical, spherical particles settling under gravity. If the particles are otherwise isolated and not influenced by other particles or boundaries, they will have equal settling velocities due to the symmetry of the induced Stokes flow. The mutual influence of the disturbance flow created by each particle leads to a settling velocity larger than that for a single isolated particle. As pointed out by Batchelor (1972) the settling velocity depends on the separation between the particles and the orientation of the line of centers to the vertical. These results are completely specified once the settling velocities are determined for two standard configurations, two spheres falling vertically parallel to the line of centers or two spheres with a horizontal separation. In both instances the particles settle vertically though this is not the case for other alignments.

The approximate, force coupling model has been used to evaluate the settling velocity of two equal spheres in these two configurations with the particle velocities evaluated by (59). The results are shown in Fig. 7. The settling velocity V is scaled as previously by the Stokes velocity W and given in terms of the distance between the centers, so $r/a = 2$ corresponds to touching spheres. The results are compared with the theoretical values quoted by Batchelor (1972) and Batchelor (1976). For larger particle separations the force coupling model gives good agreement with the exact results. The discrepancy is more noticeable for particles falling vertically along the line of centers. For two spheres in contact the force coupling model overestimates the settling velocity

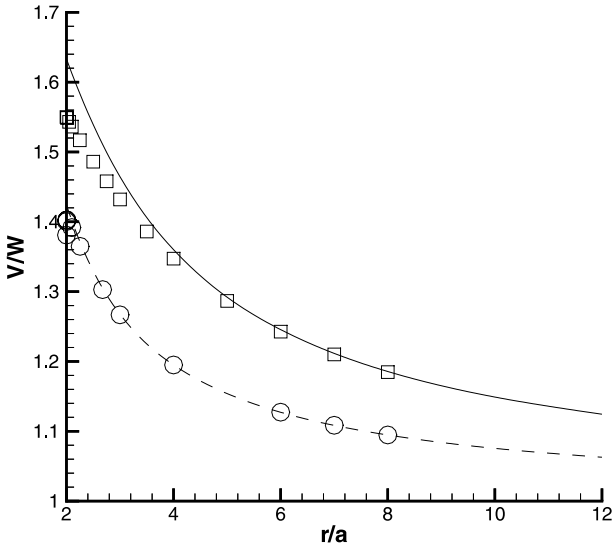

Fig. 7. Settling velocity of V of a pair of identical particles against particle separation distance r: (——) force-coupling model for vertical alignment; (- - - -) force-coupling model for horizontal alignment, (□) and (◯), corresponding results from Batchelor (1972, 1976).

giving a value of V/W equal to 1.633 compared to the correct value of 1.550, an error in absolute terms of 5%. At $r/a = 3$ the error is about 2%. These errors are due to the neglect of the higher-order multipole terms and are consistent with the values found by Ladd (1988) for lower-order multipole representations. Lubrication forces are not a factor in this example but do affect the motion of spheres settling with a horizontal separation.

For spheres with a horizontal separation the results of the force coupling model are in closer agreement with the exact results. At $r/a = 2.1$ the force coupling model gives V/W equal to 1.402 compared to the exact result of 1.392, an error of less than 1%. Lubrication forces have a strong modifying effect on the exact results between $r/a = 2.01$ and 2.0 which the model as given will not reproduce. In general there is no external torque on the particles and they are free to rotate in response to the local fluid velocity. The no-slip condition between the spheres prevents the rotation of the spheres at or near contact leading to a sharp, local change in settling velocity with $V/W = 1.380$ at $r/a = 2$. For particle suspensions at low to moderate concentrations these discrepancies are not critical.

5.3. Random suspension

The third example that illustrates the force coupling model is the application to dilute, random suspensions. Spherical particles, of equal size and weight, are seeded at random locations within a periodic domain such that none of the particles overlap. This statistically uniform array of particles then induces a Stokes flow and the velocity of each particle is evaluated from the locally averaged flow by (4). Each particle contributes to the force distribution (3) acting on the fluid with

$\mathbf{F}^{(n)}$ equal to the net weight of the particle under gravity, taking into account any buoyancy. The equation for Stokes flow

$$0 = -\nabla p + \mu\nabla^2\mathbf{u} + \mathbf{f}(\mathbf{x}, t) \tag{70}$$

together with (2) and (3) are written in terms of a Fourier series for a periodic domain of side L. The Fourier representation naturally incorporates the periodic boundary conditions and as with the example of the cubic lattice array there is no need to use an Ewald summation. For this example there was no flow evolution. For a given set of conditions, different random distribution of particles were generated to give a sample of 25 or 40 different flow fields which were then used to evaluate average settling velocities or fluctuation levels for the particle velocities. The suspension is supported by a mean pressure gradient that balances the combined force of the particles in the periodic domain. This leads to the standard normalization that there is no net volume flux in the system, the volume flux of the particles settling is countered by an equal and opposite volume flux in the fluid.

Fig. 8 shows the first set of results obtained on a mesh of 64^3 grid points and scale ratio of domain size to particle radius $L/a = 24$. These data cover the range of concentrations 0 to 15% with $c = 6\%$ correponding to a flow seeded with 200 particles. At a nominal concentration of 0% the flow consists of a single particle in a periodic array, discussed earlier in this section, and the average settling velocity $\langle V\rangle/W$ is 0.883. As the concentration increases there is an initial, almost linear decrease in $\langle V\rangle$. Following standard practice, see for example Ladd (1993), we may compare $\langle V\rangle$ to standard empirical correlations such as Richardson and Zaki (1954) by scaling the average settling velocity by the value at zero concentration V_0. Fig. 8 shows a comparison of the simulation results with the correlation

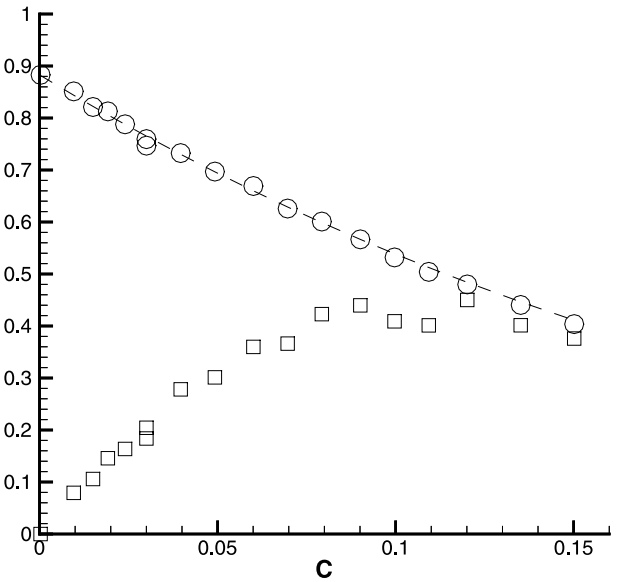

Fig. 8. Results of force-coupling model for average settling velocity $\langle V\rangle$ and mean square particle velocity fluctuations $\langle V'^2\rangle$ against concentration c: ◯, $\langle V\rangle/W$; (□), $\langle V'^2\rangle/W^2$; (----) empirical correlation (71). Domain size $L/a = 24$.

$$\langle V \rangle = V_0(1-c)^{4.7}. \tag{71}$$

There is resonable agreement and these results are consistent with experimental data such as Nicolai et al. (1995). An exponent value of 5 also yields reasonable agreement over this range.

Fig. 9 shows a second set of results obtained on a larger mesh of 128^3 grid points and the scale ratio L/a is now 48. At the nominally zero concentration level $\langle V \rangle / W = 0.941$. The same correlation (71) for the average settling velocity again gives a reasonable match with the simulation data.

The mean square particle velocity fluctuations are dominated by the vertical components. Results for these are shown too in Figs. 8 and 9 with $\langle V'^2 \rangle$ scaled by W^2. In the smaller domain the fluctuations are greatest around a particle concentration of 10% at a level of about 0.44, while in the larger domain shown in Fig. 9 the peak is about 0.85. The fluctuation levels at $c = 6\%$ are 0.36 and 0.72, respectively. This dependence of the fluctuation levels on the container size, or domain size, was demonstrated by Caflisch and Luke (1985) for simple uniform distributions of particles and is due to the long-range effect of the Stokes flow interactions between particles. The present, almost linear variation in fluctuation levels with L/a agrees with their theory. Experiments such as Nicolai et al. (1995) consistently report fluctuation levels that do not increase with container size. A number of studies and additional experiments have been carried out to determine what factors may limit the particle velocity fluctuation levels in a dynamically evolving suspension. Koch and Shaqfeh (1991) proposed a screening mechanism as one hypothesis. The recent paper by Luke (2000) summarizes the conclusions to date and in addition to possible long-range correlations in the distribution of particles proposes that stable stratification within a sedimenting suspension will have a significant effect.

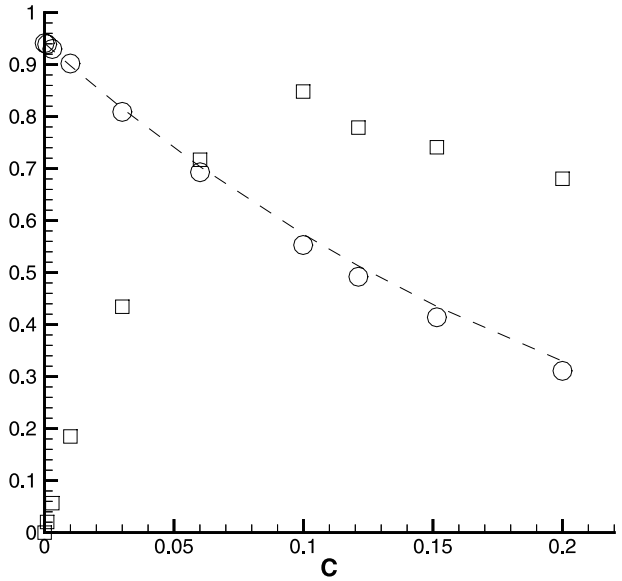

Fig. 9. Results of force-coupling model for average settling velocity $\langle V \rangle$ and mean square particle velocity fluctuations $\langle V'^2 \rangle$ against concentration c: ◯, $\langle V \rangle / W$; (□), $\langle V'^2 \rangle / W^2$; (- - - -) empirical correlation (71). Domain size $L/a = 48$.

6. Conclusion

The preceding sections illustrate how a finite force multipole expansion may be used to tackle problems in Stokes suspensions. From a computational viewpoint the finite values of all the variables and the lack of singularities mean that standard numerical methods such as fast Fourier transforms can be applied to systems involving periodic boundary conditions. More significant though is the relative ease of implementing the approximate force-coupling model involving just force monopoles. The results for the periodic cubic lattice show that quite good estimates can be obtained for overall quantities such as the sedimentation velocity even though the flow structure near an individual particle is only partially resolved. In this context these results are the same as those obtained from the Stokesian dynamics method, Brady and Bossis (1988). It is essential to account correctly for the self-induced motion of a particle and match this to the Stokes settling velocity. This is achieved by matching the particle radius to the length scale of the finite force envelope $\Delta(\mathbf{x}-\mathbf{Y})$. Once this is done consistent results can be obtained for the particle tracking and flow coupling problems that are inherent to all dispersed two-phase flow systems. Consistent energy budgets can be obtained too.

The methods described here have more general application. An example application to motion at nonzero particle Reynolds numbers is given by Dent and Maxey (2000). Indeed a major motivation of this work has been the potential use for systems of particles with low to moderate particle Reynolds numbers involving possibly unsteady flow conditions. Further results are given by Dent (1999) and Lomholt (2000).

Acknowledgements

The authors gratefully acknowledge the support provided by the National Science Foundation through the Fluid, Particulate and Hydraulic Systems Program (CTS-94-24169), the NASA-Rhode Island Space Grant Consortium and the National Center for Microgravity Research. We wish to thank Dr. Sune Lomholt of Risoe National Laboratory, Denmark and Professor Eric Climent of the University of Strasbourg, France for their assistance in the revision of this paper.

References

Batchelor, G.K., 1972. Sedimentation in a dilute dispersion of spheres. J. Fluid Mech. 52, 245–268.

Batchelor, G.K., 1976. Brownian diffusion of particles with hydrodynamic interaction. J. Fluid Mech. 74, 1–29.

Brady, J.F., Bossis, G., 1988. Stokesian dynamics. Ann. Rev. Fluid Mech. 20, 111–157.

Caflisch, R.E., Luke, J.H.C., 1985. Variance in the sedimentation speed of a suspension. Phys. Fluids 28, 759–760.

Cichoki, B., Hinsen, K., 1995. Stokes drag on conglomerates of spheres. Phys. Fluids 7, 285–291.

Dent, G.L. 1999. Aspects of particle sedimentation in dilute flows at finite Reynolds numbers. Ph.D. dissertation, Brown University, Providence RI.

Dent, G.L., Maxey, M.R., 2000. Flow through a periodic array of particles at finite Reynolds numbers. Phys. Fluids, submitted.

Elghobashi, S., Truesdell, G.C., 1993. On the two-way interaction between homogeneous turbulence and dispersed solid particles. I: Turbulence modification. Phys. Fluids A 5, 1790–1801.

Griffel, D.H., 1981. Applied Functional Analysis. Ellis Horwood, Chichester, UK.

Happel, J., Brenner, H., 1973. Mechanics of Fluids and Transport Processes. Martinus Nijhoff, Dordrecht.
Hasimoto, H., 1959. On the periodic fundamental solutions of the Stokes equations and their application to viscous flow past a cubic array of spheres. J. Fluid Mech. 5, 317–328.
Kim, S., Karrila, S.J., 1991. Microhydrodynamics: Principles and Selected Applications. Butterworth/Heinemann, London.
Koch, D.L., Shaqfeh, E.S., 1991. Screening in sedimenting suspensions. J. Fluid Mech. 224, 275–303.
Ladd, A.J.C., 1988. Hydrodynamic interactions in a suspension of spherical particles. J. Chem. Phys. 88, 5051–5063.
Ladd, A.J.C., 1993. Dynamical simulations of sedimenting spheres. Phys. Fluids A 5, 299–310.
Lighthill, M.J., 1958. Introduction to Fourier Analysis and Generalized Functions. Cambridge University Press, Cambridge.
Lomholt, M.J. 2000. Numerical investigations of macroscopic particle dynamics in microflows. Ph.D. dissertation, Risø National Laboratory, Roskilde, Denmark.
Luke, J.H.C., 2000. Decay of velocity fluctuatons in a stably stratified suspension. Phys. Fluids 12, 1619–1621.
Maxey, M.R., Patel, B.K., 1997. Force-coupled simulations of particle suspensions at zero and finite Reynolds numbers. ASME FEDSM97-3183.
Maxey, M.R., Patel, B.K., Chang, E.J., Wang, L-P., 1997. Simulations of dispersed turbulent multiphase flow. Fluid Dynamics Res. 20, 143–156.
Mazur, P., Van Saarloos, W., 1982. Many-sphere hydrodynamic interactions and mobilities in a suspension. Physica A 115, 21–57.
Mo, G., Sangani, A.S., 1994. A method for computing Stokes flow interactions among spherical objects and its application to suspensions of drops and porous particles. Phys. Fluids 6, 1637–1652.
Nicolai, H., Herzhaft, B., Hinch, E.J., Oger, L., Guazzelli, E., 1995. Particle velocity fluctuations and hydrodynamic self-diffusion of sedimenting non-Brownian spheres. Phys. Fluids 7, 12–23.
Patel, B.K., 1996. The sedimentation of spheres using a finite point-particle method. Ph.D. dissertation, Brown University, Providence, RI.
Richardson, J.F., Zaki, W.N., 1954. Sedimentation and fluidization: Part I. Trans. Inst. Chem. Eng. 32, 35–53.
Saffman, P.G., 1973. On the settling speed of free and fixed suspensions. Stud. Appl. Math. LII, 115–127.
Sangani, A.S., Acrivos, A., 1982. Slow flow through a periodic array of spheres. Int. J. Multiphase Flow 8, 343–360.
Sangani, A.S., Mo, G., 1996. An $O(N)$ algorithm for Stokes and Laplace interactions of particles. Phys. Fluids 8, 1990–2010.
Squires, K., Eaton, J.K., 1990. Particle response and turbulence modification in isotropic turbulence. Phys. Fluids A 2, 1191–1203.
Weinbaum, S., Ganatos, P., Yan, Z-Y., 1990. Numerical multipole and boundary integral equation techniques in Stokes flow. Ann. Rev. Fluid Mech. 22, 275–316.
Zick, A.A., Homsey, F.M., 1982. Stokes flow through periodic array of spheres. J. Fluid Mech. 115, 13–26.